In situ non-contact measurements of surface roughness

Yann Quinsat, Christophe Tournier

In-situ non contact measurements of surface roughness

Yann Quinsat, Christophe Tournier

LURPA, ENS Cachan, Université Paris Sud 11
61 av. du président Wilson, 94235 Cachan, France

Abstract

Surface roughness measurements are often required to validate a machining process. However, when using a 3D surface roughness measuring instruments it is usually necessary to remove the part from the machine tool between two operations, potentially introducing systematic errors. Furthermore, surface roughness measuring instruments are not suited for measuring heavy and large parts such as stamping dies. This paper presents a method to measure the surface topography of a part in-situ, i.e. directly on the machine tool without removing the part. After introducing the sensor technology and the data acquisition chain, the effects of geometric imperfections of the machine tool and compensation for thermal effects on the measurement results are discussed. An application of the method is then presented to assess a finishing process on a five-axis machining centre including milling and polishing operations.

Key words: In-situ measurements, non-contact sensor, 3D surface roughness, thermal compensation, polishing

1. Introduction

The manufacturing of molds, dies and medical implants requires the use of finishing operations such as machining and polishing so as to achieve the required surface quality. Surface roughness controls are mandatory to define the process and validate the quality of the machined part. The difficulty lies in the fact that the use of measuring instruments dedicated to 3D surface roughness measurement is limited to small parts with single orientation. Furthermore, mounting and un-mounting the part leads to systematic errors and geometrical deviations. Thus our objective is to be able to control parts of any size without removing the part from the machine tool.

According to Vacharanukul et al. [1], measurement of a part can be performed on the machine tool during the machining process (in-process measurement) or by interrupting the process and keeping the part in the part holder (in-situ measurement). Different techniques can be used for in-process and in-situ measurements [1, 2, 3]. These techniques can be categorized into six methods: mechanical, optical, pneumatic, ultrasonic, electrical and temperature detection methods. Optical techniques are often used as they provide a good compromise between acquisitions speed and axial measurement resolution. However, in-process measurement techniques must take into account the difficulties linked to the machine tool environment such as tool deflection, coolant, vibrations, etc. Grosvenor et al. [4] have investigated these difficulties within the context of in-process measurement of diameter in turning using proximity sensors. The in-process measurement method proposed by Persson [5] is based on an optical sensor using scattered light. The sensor is fixed on a grinding machine to evaluate surface roughness during grinding operations. More recently [6] this kind of sensor has been used to conduct on-line measurement on a diamond turning lathe. The sensor is fixed on a grinding machine to evaluate surface roughness during grinding operations. This measurement method may also be enriched with hybrid vision system. Tian et al. [7] have proposed to associate two digital cameras to measure laser speckle

pattern and scattering images simultaneously. Lin et al. [8] and Jiang et al. [9] have investigated the feasibility of spatial light-wave scanning to replace mechanical stylus scanning for in-situ surface roughness measurement. The developed sensor has been used for on-line nano scale surface measurement [10, 11]. However, their work has focused on the development of the sensor regardless of the interactions between the sensor and the machine and the measurement range is not compatible with the considered application.
Therefore, our approach consists in using a non contact optical sensor to achieve in-situ measurement of surface roughness on a 5-axis milling center. According to [12], a confocal chromatic sensor has been chosen. This technology is the most adapted given the five axis milling environment constraints.
The sensor is part of a MICROMESURE 3D measuring system from STIL. It is a modular measurement system including a table unit, comprising motorized x,y,z stages on which an optical pen (measuring head) is mounted and connected to a controller through an optical fiber. Within the context of in-situ measurement, the optical pen is mounted in the spindle of the machine tool with a dedicated set-up and a standard HSK 63A tool holder attachment. As the optical pen takes the place of the tool, this technique does not allow us to conduct in-process measurements.
Thus, the geometrical imperfections of the machine tool must be taken into account and the thermal expansion of the spindle has to be compensated.
The paper is organized as follows: first the sensor and the acquisition system are presented in section 2. Then in section 3, the in-situ geometrical error model is described as well as the identification of model parameters. Section 4 is dedicated to the measurement comparison between in-situ and conventional measuring system techniques. Finally, a polishing process oriented application of in-situ measurement is proposed in section 5 before concluding remarks.

2. In-situ measurement system

2.1. Non-contact sensor

The considered sensor to evaluate the surface topography is based on the chromatic confocal sensing technology from STIL [15] (figure 1). A chromatic lens L generates the image of a point white-light source as a continuum of monochromatic images. The backscattered light arrives at a pinhole P which filters out all wavelengths except a single wavelength, λ_j. The position of the focus point M is directly related to the detected wavelength λ_j.
Two different sensors have been used for our investigations. A sensor with a measuring range of 400 μm (22 nm of axial resolution), used in in-situ or in the measuring instrument and a 100 μm measuring range (5 nm of axial resolution) sensor dedicated to the measuring instrument.

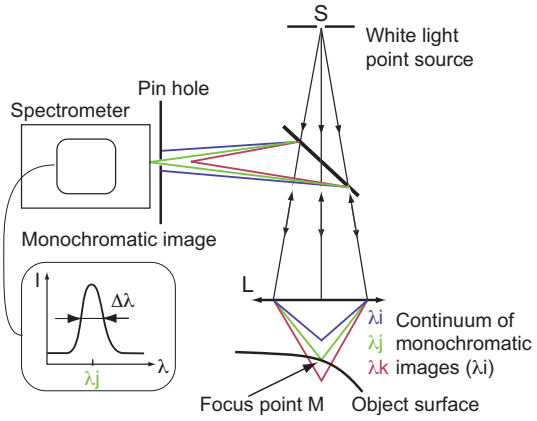

Figure 1: Non contact sensor description

2.2. Measurement procedure

The optical sensor is mounted on the machine tool spindle using a dedicated mounting system (figure 2). Thus measurements are conducted along z axis, the theoretical spindle axis of the machine tool. The sensor is connected to its dedicated controller through an optical fiber. The signal provided by the controller is recorded with an in-house visual-basic based interface.

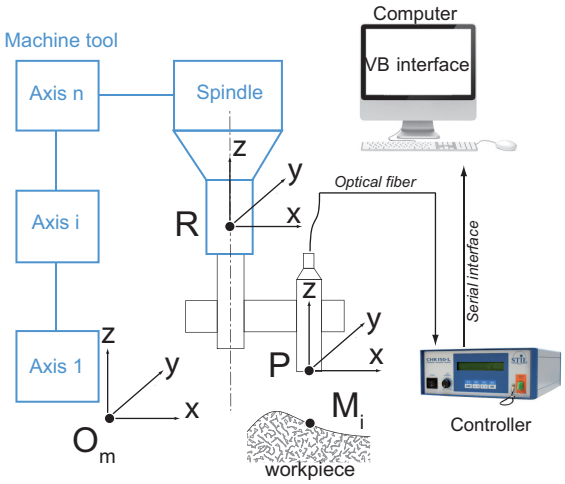

Figure 2: Measurement devices and data acquisition

The measurement is performed by a succession of 2D profile measurements along scanning paths which are parallel to a plane passing through z axis, like xz plane or yz plane for instance. The positions of the measured points in the xy plane are not monitored but computed according to the distance between scanning path and the programmed sensor displacement velocity.

2.3. Measurement geometrical modeling

As the machine tool and the system on which the sensor is mounted may present geometrical deviations, a geometrical model is proposed in order to investigate the potential source of errors. Characteristic points of the assembly are presented (figure 2) as well as the transformation matrices which model geometrical deviations.

- O_m: Origin of the machine tool measure coordinate system
- R: Characteristic point of the tool holder attachment, defined as the Reference point
- P: Origin of the optical pen measurement
- M_i: Measured point

- R_{Om}: Machine tool measure coordinate system
- R_{Rm}: Spindle coordinate system

$$M_{R_{Om}R_{Rm}} = \begin{pmatrix} & & & X \\ & I_3 & & Y \\ & & & Z \\ 0 & 0 & 0 & 1 \end{pmatrix} \tag{1}$$

- $R_{Rm\delta}$: Spindle coordinate system including machine tool geometrical deviations (straightness, squareness)

$$M_{R_{Rm}R_{Rm\delta}} = \begin{pmatrix} & & & dX \\ & R_1(\psi_1, \theta_1, \phi_1) & & dY \\ & & & dZ \\ 0 & 0 & 0 & 1 \end{pmatrix} \tag{2}$$

- $R_{Rm\Delta}$: Spindle coordinate system including machine tool geometrical deviations and thermal expansion

$$M_{R_{Rm\delta}R_{Rm\Delta}} = \begin{pmatrix} & & & \delta X \\ & R_2(\psi_2, \theta_2, \phi_2) & & \delta Y \\ & & & \delta Z \\ 0 & 0 & 0 & 1 \end{pmatrix} \tag{3}$$

- R_{Pmes}: Optical pen coordinate system

$$M_{R_{Rm\Delta}R_{Pmes}} = \begin{pmatrix} & & & a \\ & R_3(\psi_3, \theta_3, \phi_3) & & b \\ & & & c \\ 0 & 0 & 0 & 1 \end{pmatrix} \tag{4}$$

The coordinates of the point M_i in R_{Pmes} are:

$$M_i = \begin{pmatrix} 0 \\ 0 \\ h \\ 1 \end{pmatrix}_{R_{Pmes}} \tag{5}$$

$(0, 0, h, 1)$, h being the distance measured by the sensor.

- First assumption: Considering the small range of displacement during measurements, it has been stated that:

  $$R_1(\psi_1, \theta_1, \phi_1) = I_3 \text{ and } dX = dY = dZ = 0$$

  This assumption amounts to considering that the axes straightness is perfect along the small displacement. It is also assumed that the axes squareness is a second order error compared to the thermal deviation.

- Second assumption: measurement duration is supposed to be short compared to the thermal inertia of the machine tool structure. The thermal expansion of the spindle due to its cooling system is considered to be more significant. Spindle expansions leading to small rotations and expansions in the x and y directions are neglected:

  $$R_2(\psi_2, \theta_2, \phi_2) = I_3 \text{ and } \delta X = \delta Y = 0$$

- Third assumption: the pen sensor is supposed to be collinear to the spindle axis which leads to state that:

  $$R_3(\psi_3, \theta_3\phi_3) = I_3$$

  This hypothesis consists in neglecting the altitude measurement error (cosine error) which is a second order error.

These assumptions also mean that the position of the measured point in the xy plane remains unknown. However, the distance between two measurement

lines is constant. This should have small consequences on the 3D roughness parameter values. This point is validated in section 4.
Then, the coordinates of the point M_i in R_{Om} are the following:

$$M_i = \begin{pmatrix} X + a \\ Y + b \\ Z + \delta Z + c + h \\ 1 \end{pmatrix}_{R_{Om}} \tag{6}$$

3. Model identification

The model outlined above is only a geometrical model. The term δZ corresponding to the spindle expansion and the z axis repeatability of the machine tool needs to be identified.

3.1. Thermal behavior

The machine tool spindle is cooled by an air conditioning system so as to maintain a limited operating temperature. Thus, expansions of the spindle are contained in a range proportional to the temperature variation of the coolant ($20\ C^\circ \pm 1$). As these expansions have an impact on the in-situ measurement, they need to be known. In order to take into account the existence of measurement variations due to thermal expansion, the same point on a polished surface has been measured without moving the sensor during 100 min. The acquisition frequency of measurements was set to 1 kHz (figure 3). In parallel, the cooling cycle of the spindle has been recorded in order to establish a compensation model for measuring defects. Temperature variations of the coolant, of the nose of the spindle as well as the ambient temperature have been recorded during the measurement (figure 4).
Variations obtained during the measurement period clearly show the cyclical nature of the thermal behavior. As every first order system, temperature is following cycles of exponential functions, but in order to simplify the data interpolation, a sinusoidal model has been chosen $T(t)$:

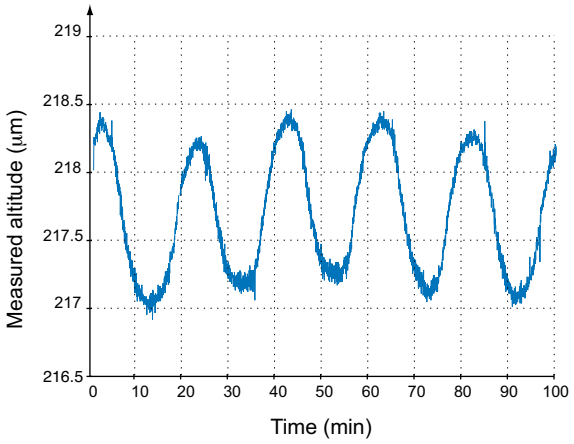

Figure 3: Measurement of a given point during 100 min

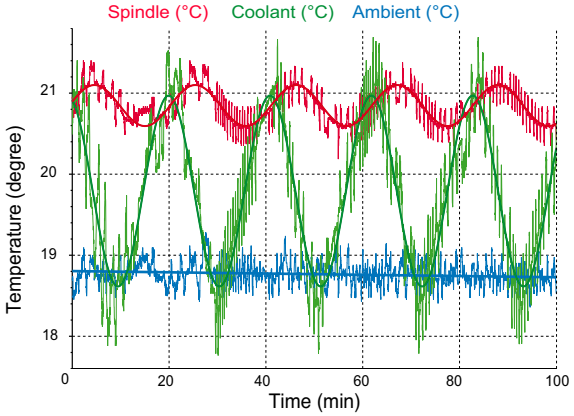

Figure 4: Temperatures monitoring

$$T(t) = A.sin(B.t + C) + D \tag{7}$$

Sinusoidal functions associated with the two evolution curves of the fluid temperature and of the spindle are defined in table 6.

The frequency B of the two curves is identical and corresponds to a period of 20 min. A phase shift between the two curves due to heat transfer by conduction is also observed. With these curves, the thermal effects due to cooling cycle can be compensated. The thermal effects compensation allows us

	A	B	C	D
Coolant	0.2531	0.301	0.1876	20.85
Spindle	1.177	0.300	0.1877	19.79

Table 1: Thermal behavior

to conduct a study on the influence of the repeatability of the machine tool.

3.2. Z-axis repeatability study

The purpose of this section is to determine the influence of the z axis repeatability of positioning on measurement results. According to ISO 230-2 [13], a series of measurements of three points M_i in three different locations of the z axis (spaced 100 mm) has been conducted. Each point has been measured 650 times. For each measurement m_{ij}, the measurement frequency is fixed to 1 kHz for a period of 4 s. The measurement cycle is thus composed of a slow approach (20 mm/min) over a 1 mm downward displacement along z axis, the measurement, and a fast retract (200 mm/min).
After the compensation of the thermal effect, measured values z_{ij} are normally distributed (figure 5) and the estimators of standard uncertainty in the downward direction $s_i \downarrow$ are equal to 0.0704 μm, 0.1044 μm and 0.0714 μm. This leads to a repeatability of positioning $R \downarrow$ equal to 0.328 μm
($R \downarrow = \max(4.s_i \downarrow)$.
The conclusion of this study is that below 0.3 μm, measurement uncertainty becomes too important to evaluate geometrical deviations.

4. Model validation

The proposed measurement model (eq.6) consists in neglecting most of the geometrical defects (assumptions 1,2 and 3) of the machine tool. In order to validate the method and the measurement model, two parts have been measured with the same sensor on the machine tool and on the dedicated measuring system.

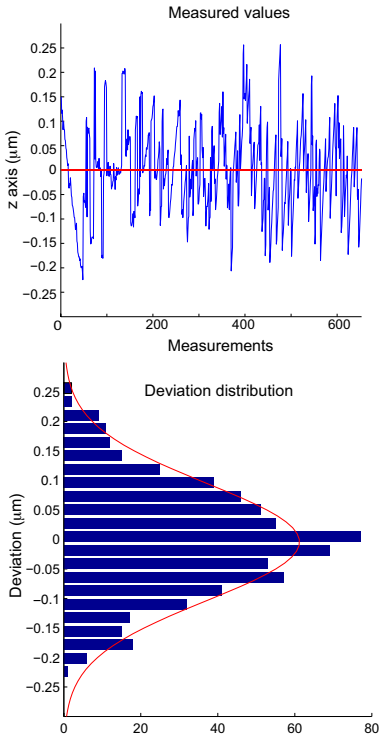

Figure 5: Z-axis repeatability (point M_1)

4.1. Single groove measurement

The first part to be measured presents a calibrated groove (1 μm depth, 100 μm width) on a polished plane (ISO 12179 type A artefact [14]). This calibrated groove has been chosen to validate the assumptions regarding the misalignment of the sensor compared to the z axis and the geometrical errors of the machine tool (straightness and squareness). Both sensors have been employed on the measuring system or in-situ leading to three different measurement configurations. Groove measurement results are gathered in table 2 and in figure 6. Values reported in table 2 are computed in the central orange area of figure 6. It can be observed that the in-situ measurement is very noisy compared to the others. The same artifacts are visible on both sides of the groove for 22 nm sensor due to sensor saturation, which could not be corrected on the used sensor. However, the groove depth result for in-situ

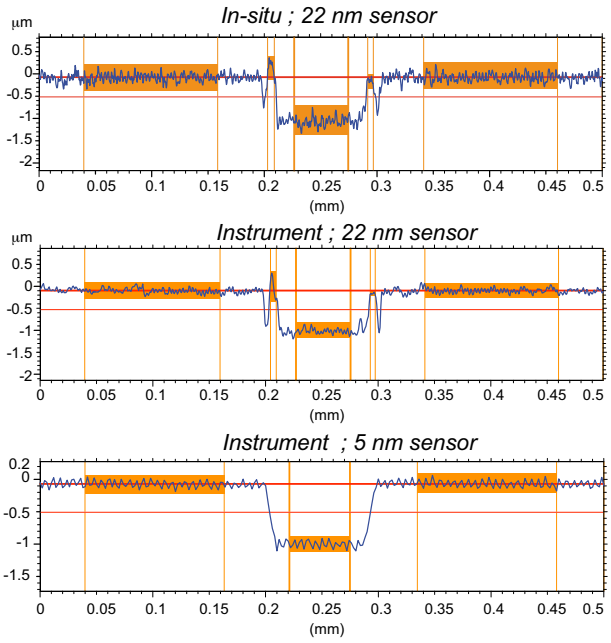

Figure 6: Measured groove profiles

configuration fits to the calibrated depth. Furthermore, since the result for in-situ measurement is consistent with the calibrated depth of the groove, the orientation of the optical pen is aligned with the z axis, which validates the assumptions leading to neglect the rotation matrices $R_i(\psi_i, \theta_i, \phi_i)$. It also shows that the measurement noise generated during machine tool displacement is normally distributed as there is no significant slope. This is a first validation showing that the straightness deviations of the x and y axes are also insignificant.

	Groove depth
In-situ 22 nm sensor	$\bar{x} = 0.999\ \mu$m
Instrument 22 nm sensor	$\bar{x} = 0.919\ \mu$m
Instrument 5 nm sensor	$\bar{x} = 0.931\ \mu$m

Table 2: Groove measurement results

4.2. Complex topography measurement

The surface belongs to a roughness sample presenting a certified 2D arithmetic roughness Ra equal to 2.97 μm. It has been used to validate straightness along x and y axes ($dX = dY = 0$) and thermal distortion along x and y axes ($\delta X = \delta Y = 0$). The in-situ measurement is compared to measuring instrument measurement through the evaluation of several roughness parameters, Ra, Sa and St [15] (table 6). The first two parameters are mean parameters whilst the last one is a maximum value parameter. The error in the evaluation of Ra and Sa is about 10 % and is probably due to the larger spot size of the 22 nm optical pen that produces a local averaging. Regarding the evaluation of St, results with the 22 nm sensor are twice as large as the result given by the 5 nm sensor. The higher resolution 5 nm sensor has a higher spatial resolution, seeing more details, leading to somewhat higher averaging parameters like Ra and Sa. The peak parameter St becomes on the contrary smaller for the higher resolution sensor, because it produces fewer edge effects on the rough surface, which are evident on the groove profiles in figure 6.
It shows that it is possible to measure correctly complex topography although the measured point in the xy plane is never known exactly. However, it seems that the machine tool does not introduce large straightness deviations compared to the measuring instrument. According to the results of the two sample measurements, the three assumptions stated in 2.3 seem to be validated for the application.

	Ra μm	Sa μm	St μm
In-situ 22 nm	2.61	2.69	22.6
Instrument 22 nm	2.75	2.79	25.2
Instrument 5 nm	3.00	3.01	12.5

Table 3: Topography measurement results

5. Application

The proposed application deals with the finishing operation of a plane surface. By using in-situ measurement, it is possible to know when the surface roughness of the part has been reduced to the desirable level. The plane is machined in a 50 mm × 50 mm section block made of X38CrMoV5 steel. The part is machined on a 5-axis Mikron UCP710 machine tool to reach a milling finishing state before polishing. Three different grades of abrasive have been used for rough polishing operations (grade 120, 240 and 600). Abrasives are 18 mm diameter disks of silicon carbide pasted on the flexible support [16]. The polishing operations were carried out with a tilt angle of the tool in the feed direction equal to 10°. Surface roughness has been measured in-situ after each of the five operations using the proposed method. Measurements have been carried out in a restricted area (4 mm × 1 mm) of the machined plane and with a scanning direction perpendicular to the tool path (figure 7, 8-12).

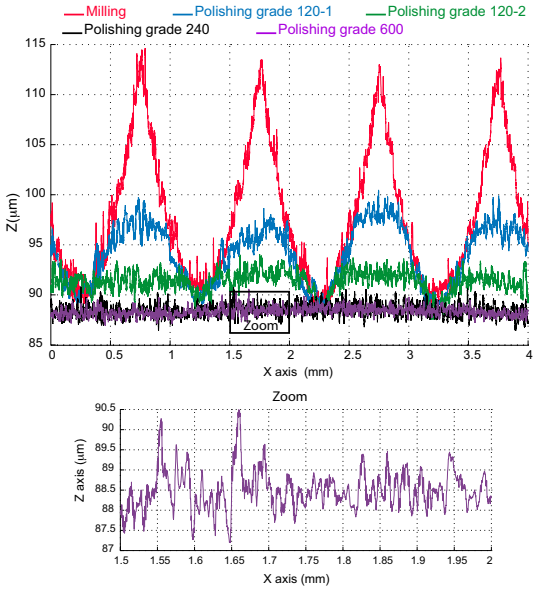

Figure 7: In-situ measurement 2D profiles

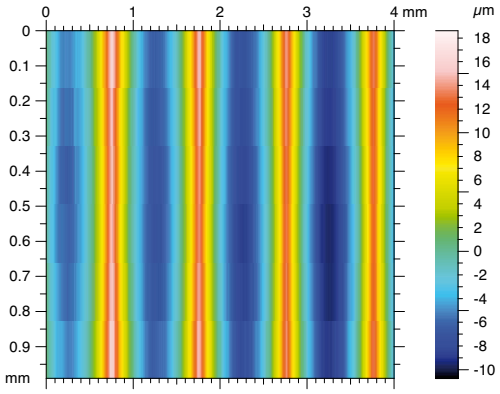

Figure 8: In-situ measurement ; Milling

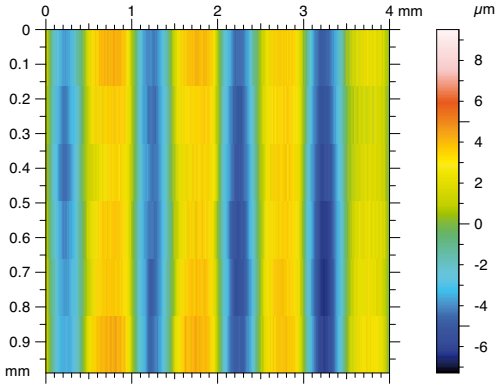

Figure 9: In-situ measurement ; Grade 120-1

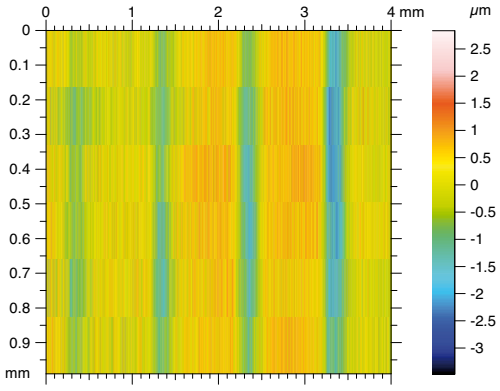

Figure 10: In-situ measurement ; Grade 120-2

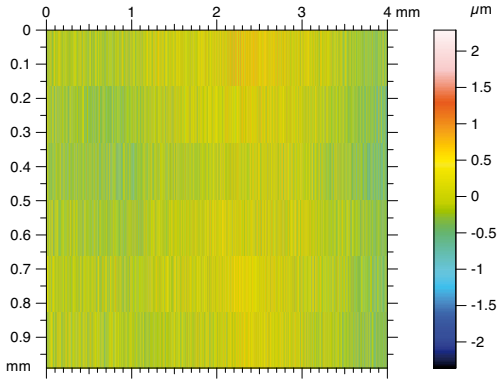

Figure 11: In-situ measurement ; Grade 240

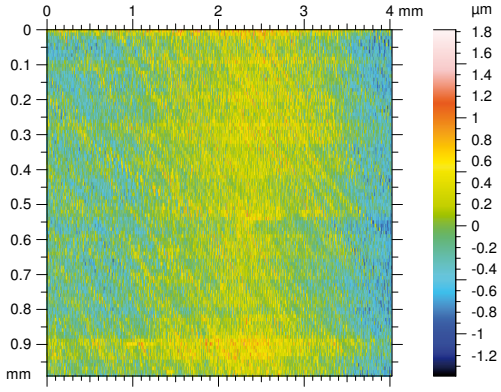

Figure 12: In-situ measurement ; Grade 600

Regarding the machining operation, the scallops generated by the ball-end tool are clearly visible. The removal of the scallops begins with the first abrasive tool (grade 120, path-1). After the second abrasive tool (grade 120, path-2), most of the scallops have disappeared and some valleys remain on the part. The grade 240 abrasive removes all the valleys and the amplitude of the geometrical deviations are close to 5 μm. The last abrasive paper (grade 600) generates smaller deviations (3 μm) as can be seen in the zoom area with some details of about 0.5 μm. Beyond this value, it may be difficult to distinguish the part roughness from the noise of the instrument.

6. Conclusion

The purpose of this paper was to introduce a method for measuring surface roughness in-situ, i.e. on the machine without removing the part. A study of the thermal effects of the cooling cycle of the spindle on which the sensor is mounted enabled compensation of most of the effects due to thermal expansion. The results of different experiments show that the stability of the machine tool leads to the largest errors, especially regarding the repeatability. However, it is quite possible to measure the evolution of surface roughness during milling and polishing operations in order to optimize the processes. Geometrical deviations down to 0.5 μm can be measured, which is approximately the limit that abrasive paper can reach before diamond paste polishing is required.

References

[1] K. Vacharanukul and S. Mekid, In process dimensionnal inspection sensors. Measurement 2005;38(3):204-218.

[2] T. Yandayan and M. Burdekin. In-process dimensional measurement and control of workpiece accuracy. International Journal of Machine Tools and Manufacture 1997;37(10):1423-1439.

[3] M. Shiraishi, Scope of in-process measurement, monitoring and control techniques in machining processes-part 2: Inprocess techniques for workpieces. Precison Engineering 1989;11(1): 27-37.

[4] R. I. Grosvenor, C. Kharpoutly, and K. F. Martin, In-process measurement problems in machine tool applications. International Journal of Production Research 1991;29(2):357-374.

[5] U. Persson. In-process measurement of surface roughness using light scattering. Wear 1998;215(1-2):54-58.

[6] S. Wang, Y. Tian, C.J. Tay and C. Quan. Development of a laser-scattering-based probe for on-line measurement of surface roughness. Applied Optiques 2003;42(7):1318-1324.

[7] G. Y. Tian and R. -S. Lu, Hybrid vision system for online measurement of surface roughness. Journal of Optical Society of America 2006;23(12):3072-3079.

[8] D. Lin, X. Jiang, F. Xie W. Zhang, L. Zhang and I. Bennion. High stability multiplexed fibre interferometer and its application on absolute displacement measurement and on-line surface metrology. Optics Express 2004;23(12):5729-5734.

[9] X. Jiang, D. Lin, L. Blunt, W. Zhang, and L. Zhang. Investigation of some critical aspects of on- line surface measurement by a wavelength-division-multiplexing technique. Measurement Science and Technology 2006;17(3):483-487.

[10] K. Wang, H. Martin and X. Jiang. Actively stabilized optical fiber interferometry technique for online/in-process surface measurement. Review of scientific instruments 2008; 79(2). ISSN 0034-6748.

[11] S. Yang, X. Jiang, G. Maxwell and K. Wang. An integrated optical coupler used in a fibre interferometry system for on-line surface measurements. Optics Communications 2008;281:1099-1107.

[12] U. Minoni and F. Cavalli. Surface quality control device for on-line applications. Measurement 2008;41:774-782.

[13] ISO 230-2: 2006 Test code for machine tools – Part 2: Determination of accuracy and repeatability of positioning numerically controlled axes.

[14] ISO 12179: 2000 Geometrical product specification (GPS) - Surface texture: protocole method - Calibration of contact (stylus) instruments.

[15] R. K. Leach, Fundamental Principles of Engineering Nanometrology, Elsevier, 2010.

[16] X. Pessoles and C. Tournier. Automatic polishing process of plastic injection molds on a 5-axis milling center. Journal of Materials Processing Technology 2009;209(7):3665-3673.

Figure 1: Non contact sensor description

Figure 2: Measurement devices and data acquisition

Figure 3: Measurement of a given point during 100 min

Figure 4: Temperatures monitoring

Figure 5: Z-axis repeatability (point M_1)

Figure 6: Measured groove profiles

Figure 7: In-situ measurement 2D profiles

Figure 8: In-situ measurement ; Milling

Figure 9: In-situ measurement ; Grade 120-1

Figure 10: In-situ measurement ; Grade 120-2

Figure 11: In-situ measurement ; Grade 240

Figure 12: In-situ measurement ; Grade 600

	A	B	C	D
Coolant	0.2531	0.301	0.1876	20.85
Spindle	1.177	0.300	0.1877	19.79

Table1: Thermal behavior

	Groove depth
In-situ 22 nm sensor	$\bar{x} = 0.999$ μm
Instrument 22 nm sensor	$\bar{x} = 0.919$ μm
Instrument 5 nm sensor	$\bar{x} = 0.931$ μm

Table 2: Groove measurement results

	Ra μm	Sa μm	St μm
In-situ 22 nm	2.61	2.69	22.6
Instrument 22 nm	2.75	2.79	25.2
Instrument 5 nm	3.00	3.01	12.5

Table3: Topography measurement results